Materials Letters 309 (2022) 131416

Contents lists available at ScienceDirect

Materials Letters

journal homepage: www.elsevier.com/locate/matlet

Thermoelectric properties of medium-entropy PbSbTeSe alloy prepared by reactive spark plasma sintering

Ekaterina Yaprintseva [a], Alexei Vasil'ev [a], Maxim Yaprintsev [b], Oleg Ivanov [a,*]

[a] Belgorod State Technological University named after V.G. Shukhov, Belgorod 308012, Russian Federation
[b] Belgorod State University, Belgorod 394015, Russian Federation

ARTICLE INFO

Keywords:
Medium-entropy alloys
Reactive spark plasma sintering
Self-propagating high-temperature synthesis
Thermoelectric properties

ABSTRACT

Reactive spark plasma sintering combining the synthesis and densification stages has been at the first time applied to prepare medium-entropy grained PbSbTeSe alloy. This alloy is prospect medium-temperature *p*-type thermoelectric. Self-propagating high-temperature synthesis in initial mixture of elemental Pb, Sb, Te and Se powders, resulting in synthesis of single-phased PbSbTeSe, was stage of synthesis. Lattice thermal conductivity of the alloy is very low (~0.7 at ~ 755 K). Owing to this low lattice thermal conductivity, thermoelectric performance of PbSbTeSe alloy is promising . Highest thermoelectric figure-of-merit equal to ~ 0.43 is observed at ~ 720 K. Anomalies of thermoelectric properties were found at ~ 490 K. These anomalies can be related to specific features of energy bands, consisting of two valence bands, which are close in energy.

1. Introduction

Aim of this work is to prepare medium-entropy PbSbTeSe alloy by reactive spark plasma sintering (RSPS), which includes self-propagating high-temperature synthesis (SHS), and analyze features in thermoelectric properties of this alloy. Developing high-entropy (consisting of five or more principal elements in equimolar or near-equimolar ratio, which competes for the same position in crystal lattice) and medium-entropy (consisting of three or four principal elements) alloys is effective approach in modern materials science [1–3]. Due to effects of high-mixing entropy and chemical complexity, these alloys show unique properties. Particularly, the alloys possess intrinsically low lattice thermal conductivity, originated from scattering of phonons by lattice disorder. Medium-entropy PbSbTeSe alloy is prospect *p*-type thermoelectric [4]. Usually, to sinter bulk material from relevant initial powder, synthesis of initial powder (stage I) and densification of powder during sintering bulk material (stage II) are carried out separately by using different technological processes. As result, several processes of long-time sintering and multiple re-sintering, crushing and washing are involved. Preparation of material becomes complex and time-consuming. Material can be contaminated during this multi-staged fabrication, which will crucially affect reproducibility of its properties. The I and II stages can be unified into single process by using RSPS-process. Under RSPS-process, the synthesis and densification stages are implemented as two successive or parallel stages in single technological process [5]. As synthesis stage, self-propagating high-temperature synthesis (SHS) can be involved. SHS is self-sustained combustion, based on synthesis from elemental powders, reactions of solid compounds, thermite-type reactions and combustion of porous solid reactive media in a gaseous oxidizer [6]. Combination of SPS- and SHS-processes into RSPS-process allows synthesizing materials with desired structure and composition for very short time, shortening densification time, lowering sintering temperature and fabricating dense bulk material.

2. Material and methods

To prepare PbSbTeSe alloy, initial mixture of elemental Bi, Sb, Se and Te was thoroughly mixed by ball mill. This mixture was RSPS-treated by SPS 25/10 system. Tuning parameters of RSPS-process, material with desired phase composition and crystal structure can be synthesized via SHS, and bulk samples can be sintered at densification stage. Density of bulk samples was measured by Archimedes method. To find onset temperature of SHS for initial mixture of Pb, Sb, Te and Se powders, differential thermal analysis (DTA) was performed with SDT Q600 thermal analyzer in Ar atmosphere at rate of 10 K/min using α-Al_2O_3 powder as reference. To identify crystal structure and phase composition of samples, X-ray diffraction (XRD) analysis was carried out by Rigaku Ultima IV diffractometer with CuK_α-radiation. To examine

* Corresponding author.
E-mail address: Ivanov.Oleg@bsu.edu.ru (O. Ivanov).

https://doi.org/10.1016/j.matlet.2021.131416
Received 30 September 2021; Received in revised form 25 November 2021; Accepted 30 November 2021
Available online 3 December 2021

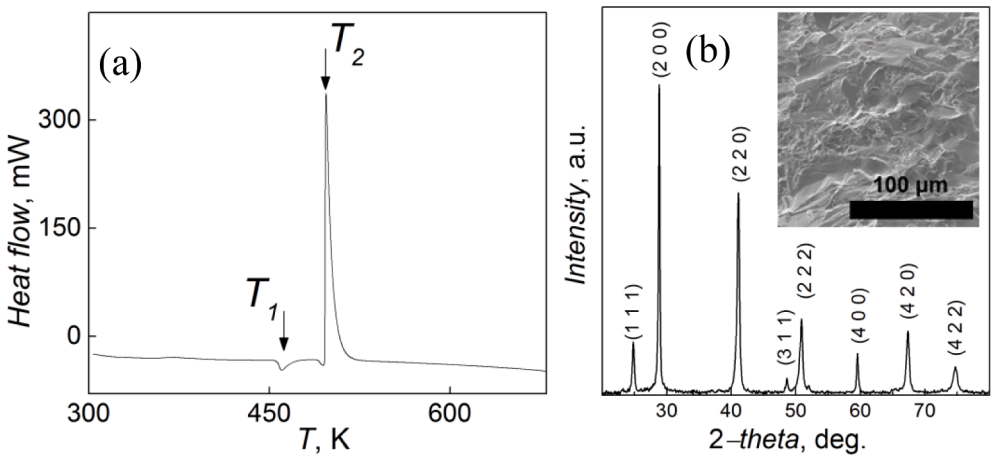

Fig. 1. (a) DTA curve taken at heating of mixture of elemental Pb, Sb, Te and Se powders; (b) XRD pattern of material after RSPS-process of mixture of Pb, Sb, Te and Se powders. Inset is SEM image of fractured surface of material.

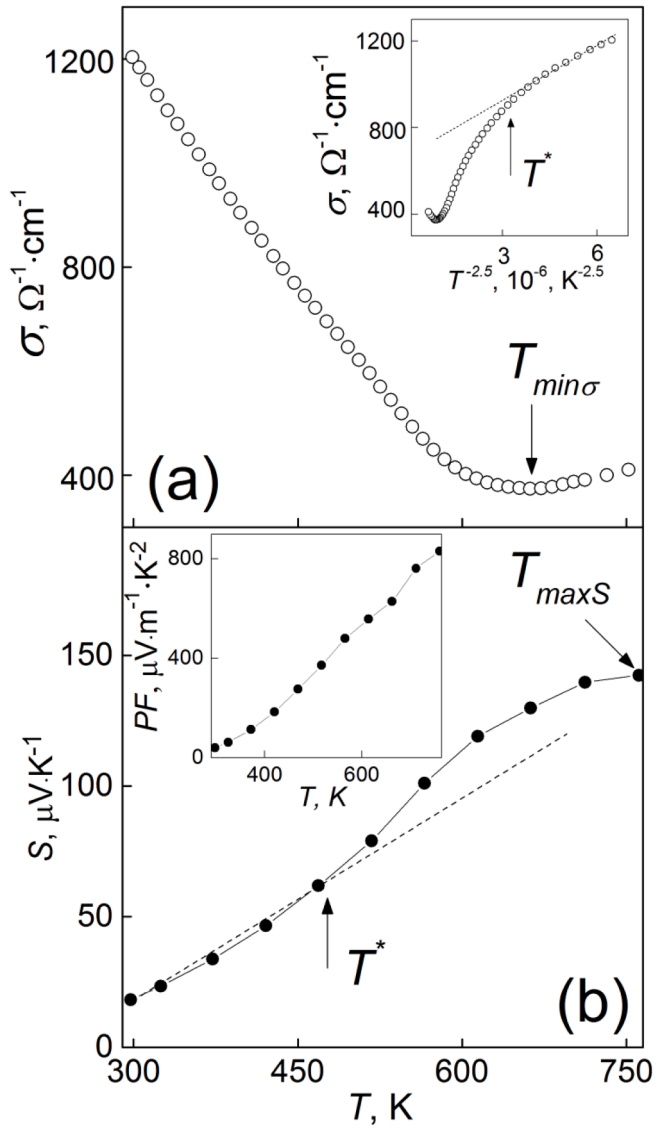

Fig. 2. The σ(a) and S (b) vs. T dependences. Inset (a) is the σ vs. $T^{2.5}$ dependence, and inset (b) is the PF vs. T dependence.

microstructure of samples, scanning electron microscopy (SEM, Nova NanoSEM 450 microscope) was applied. Elemental composition of samples was determined by energy dispersive X-ray spectroscopy (EDS) method. Specific electrical conductivity, σ, and Seebeck coefficient, S, were measured by using ZEM-3 system, and total thermal conductivity, k, was measured by TC-1200 system. A Mini Cryogen Free Measurements System (Cryogenic Ltd) was also used to study Hall effect and estimate concentration, n, and Hall mobility, μ_H, of majority charge carriers.

3. Results and discussion

Key technological parameter of SHS is its onset temperature. To find this temperature for mixture of Pb, Sb, Te and Se powders, DTA curve was taken under heating of mixture (Fig. 1 (a). Two thermal processes are observed. First weak endothermic process at temperature $T_1 \approx 460$ K is related to melting Se in powder mixture, whereas second powerful exothermic process at temperature $T_2 \approx 500$ K is originated from synthesis of PbSbTeSe due to SHS. By correct tuning technological variables, SHS can be implemented as first stage of RSPS-process. To include SHS in common SPS-process and transfer to RSPS-process, technological regime was applied as follows. Initial mixture of Pb, Sb, Te and Se powders was filled into graphite cylindrical die, which was put in chamber of SPS 25/10 system and undergone uniaxial 20 MPa pressuring in vacuum. Pulse 1500 A current was simultaneously passed through die for 2–3 s. Onset of SHS was recorded by abrupt increasing in powder mixture temperature and simultaneous shrinking material being synthesized. Then the material was heating to 823 K under the same pressure and holding at this temperature for 15 min. Therefore, both synthesis of PbSbTeSe compound and densification of this compound are two successive stages of single RSPS-process.

In accordance with XRD data (Fig. 1 (b)), RSPS-treated material is single-phased and corresponds to cubic $Fm\bar{3}m$ structure with lattice $a =$ 0.6216 nm parameter. This structure is characteristic for PbSbTeSe alloy [4]. No traces of other phases are observed. In accordance with SEM data (inset to Fig. 1 (b)), bulk PbSbTeSe sample is grained and consists of irregularly-shaped grains with size of several dozens of nm. Density of samples is ~ 7.07 g cm^{-3} that is in agreement with data reported in Ref. [4]. According to results of EDS, elemental composition of sample corresponds to PbSbTeSe composition. All elements are distributed homogeneously excluding Te, which is accumulated as small Te excess at grain boundaries.

The $\sigma(T)$ and S(T) dependences of are shown in Fig. 2 (a) and (b), respectively. The $\sigma(T)$ minimum is observed at $T_{min\sigma} \approx 670$ K. Below the minimum, σ is gradually decreasing with increasing temperature. This

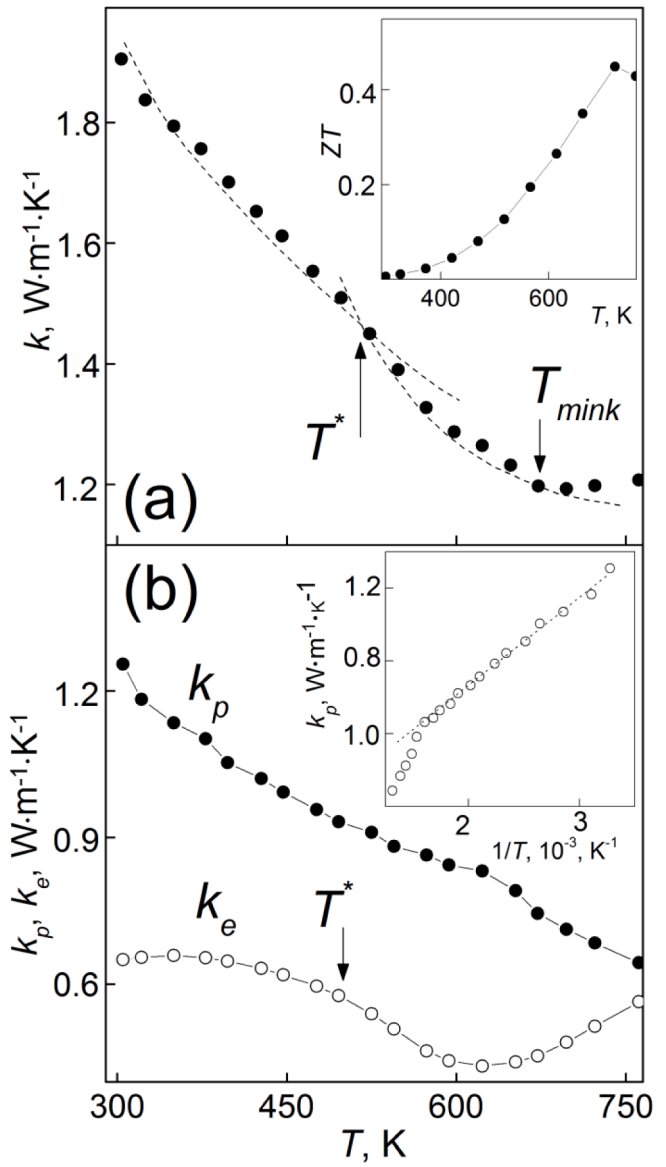

Fig. 3. The k (a), and k_p and k_e (b) vs. T dependences. Inset (a) is the ZT vs. T dependence, and inset (b) is the k_p vs. T^{-1} dependence.

$\sigma(T)$ behavior is observed in metals and degenerate semiconductors. Conductivity of p-type semiconductor is given by $\sigma = e\mu_P p$, where e, μ_P and p are unit charge, mobility and concentration of holes, respectively. Using Hall effect examination, μ_P and p were estimated as 150 $cm^2 \cdot V^{-1} \cdot s^{-1}$ and $5 \cdot 10^{19}$ cm^{-3}, respectively. For degenerate semiconductors, p is T-independent, i.e. the $\sigma(T)$ changes, corresponding to degenerate semiconductor behavior in Fig. 2 (a), is related to changes in $\mu_P(T)$. Above room temperature, carriers scattering by acoustic and optical phonons is dominant mechanism that contributes into $\mu_P(T)$ behavior. Empirical expression for this mechanism is given as $\mu_P \sim T^{-m}$, where m is exponent, changing from 1.5 to 2.5. For low temperatures, experimental $\sigma(T)$ curve is fitted in the best manner with $m = 2.5$ (inset to Fig. 2 (a)). Above temperature $T^* \approx 490$ K, fitting dashed line starts to deviate from the experimental curve. Minimum of $\sigma(T)$ is related to onset of intrinsic conductivity, resulting in increasing σ via thermal excitation of carriers from valence band to conduction band.

Seebeck coefficient is positive that corresponds to p-type conductivity (Fig. 2 (b)). At heating, S firstly increases, but at high temperatures S trends to constant value. Actually, $S(T)$ curve corresponds to left part of broad $S(T)$ maximum positioned at $T_{maxS} \approx 760$ K, which is originated from intrinsic conductivity. Behavior of $S(T)$ for degenerate semiconductor obeys $S \sim T$ link. This link, shown by dashed line, can be applied to describe experimental $S(T)$ curve only below T^*. The $\sigma(T)$ and $S(T)$ data were further used to calculate power factor, $PF = S^2 \cdot \sigma$. (inset to Fig. 2 (b)). With increasing temperature, PF increases. The $S(T)$ dependence was applied to estimate band gap, E_g. In accordance with the Goldsmid-Sharp expression, E_g, maximum value of Seebeck coefficient ($|S|_{max}$) and temperature at which it occurs (T_{max}), are related by expression $E_g = 2e|S|_{max}T_{max}$ [7]. This expression results in E_g estimate, equal to ~ 0.22 eV.

The $k(T)$ dependence is shown in Fig. 3 (a). With increasing temperature, k is reducing, trending to minimum at $T_{mink} \approx 670$ K. Kink in the $k(T)$ dependence is observed at T^*. To clearly show the kink, dashed curves above and below T^* were drawn as guides to the eyes. Lattice thermal conductivity, k_p, electronic thermal conductivity, k_e, and bipolar thermal conductivity, k_b, contribute into k. Contribution from k_b is responsible for growing $k(T)$ dependence above T_{mink}. Contribution from k_e is related to specific electrical conductivity through the Wiedemann-Franz law, $k_e = L\sigma T$, where L is Lorenz number. Using relation $L[10^{-8}, W \cdot \Omega \cdot K^{-2}] = 1.5 + \exp(-|S|_{max}\ [\mu V \cdot K^{-1}]/116)$ [8], value of L was estimated as 1.79×10^{-8} $W \cdot \Omega\ K^{-2}$. Contribution from k_e, calculated by the Wiedemann-Franz law, and contribution from k_p, calculated as $k_p(T) = k(T) - k_e(T)$, are shown in Fig. 3 (b). At heating above Debye temperature, k_p is varied as T^{-1}. The $k_p(T^{-1})$ dependence is shown in inset to Fig. 3 (b). From room temperature to T_{mink}, this dependence is linear. Lattice thermal conductivity is very low (~0.7 at ~ 755 K). Low k_p is specific feature of high-entropy and medium-entropy alloys. Contribution from k_e changes in complicated manner, especially near temperatures T^* and T_{mink}.

The $\sigma(T)$, $S(T)$ and $k(T)$ dependences were used to extract temperature dependence of thermoelectric figure-of-merit, $ZT = (TS^2\sigma)/k$ (Fig. 3 (a)). With increasing temperature, ZT increases and reaches maximum ~ 0.43 value at ~ 720 K.

New finding of our work is observation of anomalies in thermoelectric properties of PbSbTeSe at temperature T^* (T^*-anomalies). These anomalies can be attributed to an intrinsic electronic property characteristic for PbTe and SnSe, which can be related to the presence of a second valence band close in energy to the primary one [9]. With increasing temperature, thermal generation of holes from valence bands will affect electrical and thermal conductivities and Seebeck coefficient. To clear nature of T^*-anomalies, further experimental work is in progress now.

4. Conclusion

Thus, RSPS-process including SHS stage was successfully applied to prepare medium-entropy single-phased PbSbTeSe alloy. Owing to its low lattice thermal conductivity, thermoelectric performance of the alloy is promising. Next step should be transition from this four-element medium-entropy PbSbTeSe alloy to five- or six-element high-entropy alloy based on precursor PbSbTeSe system.

CRediT authorship contribution statement

Ekaterina Yaprintseva: Investigation. **Alexei Vasil'ev:** Investigation. **Maxim Yaprintsev:** Conceptualization. **Oleg Ivanov:** Conceptualization, Writing – review & editing.

Declaration of Competing Interest

The authors declare that they have no known competing financial interests or personal relationships that could have appeared to influence the work reported in this paper.

Acknowledgements

This work was supported by Ministry of Science and Higher Education of the Russian Federation (grant number No 0625-2020-0015). All of studies were carried out by the scientific equipment of joint research centre "Technologies and Materials" at the Belgorod State University.

References

[1] S. Shafeie, S. Guo, Q. Hu, H. Fahlquist, P. Erhart, A. Palmqvist, J. Appl. Phys. 118 (184905) (2015) 1–10.
[2] O. Ivanov, M. Yaprintsev, A. Vasil'ev, E. Yaprintseva, J. Alloys Compd. 872 (159743) (2021) 1–7.
[3] X.-L. Shi, J. Zou, Z.-G. Chen, Chem. Revs. 120 (2020) 7399–7515.
[4] Z. Fan, H. Wang, Y. Wu, X. Liu, Z. Lu, Mater. Res. Lett. 5 (2017) 187–194.
[5] A. Novitskii, G. Guélou, D. Moskovskikh, A. Voronin, E. Zakharova, L. Shvanskaya, A. Bogach, A. Vasiliev, V. Khovaylo, T. Mori, J. Alloys Compd. 785 (2019) 96–104.
[6] E.A. Levashov, A.S. Mukasyan, A.S. Rogachev, D.V. Shtansky, Int. Mater. Rev. 60 (2017) 203–239.
[7] H.J. Goldsmid, J.W. Sharp, J. Electron. Mater. 28 (1999) 869–872.
[8] H. Kim, Z. Gibbs, Y. Tang, H. Wang, G. Snyder, APL Mater. 3 (041506) (2015) 1–5.
[9] D. Parker, X. Chen, D.J. Singh, Phys. Rev. Lett. 110 (146601) (2013) 1–5.